ACTA METALLURGICA SLOVACA
2022, VOL. 28, NO. 3, 140-146

RESEARCH PAPER

ANALYSING EFFECT OF QUENCHING AND TEMPERING INTO MECHANICAL PROPERTIES AND MICROSTRUCTURE OF 304-SS WELDED PLATES

Saurabh Dewangan[1], Somnath Chattopadhyaya*[2]

[1]Department of Mechanical Engineering, Manipal University Jaipur, Jaipur, Rajasthan, India, Pin-303007
[2]Department of Mechanical Engineering, Indian Institute of Technology (ISM) Dhanbad, Jharkhand, India, Pin-826004

*Corresponding author: saurabh22490@gmail.com, tel.: 0141-3999100-838, Manipal University Jaipur, 303007, Jaipur, Rajasthan, India

Received: 18.07.2022
Accepted: 12.09.2022

ABSTRACT

The present work deals with analysis of mechanical performance and microstructural appearance of quenched and tempered SS-304 welded joints made by MIG welding technique. Since welding involves a critical solidification and thereby lots of internal stresses. Hence, heat treatment becomes important for removing stresses and grain refinement. In the present work, two SS-304 welded plates were heat treated. First plate was in quenched condition, and another was in tempered state. In both the plates, mechanical properties like tensile strength, impact strength, and hardness were analyzed. In addition, the microstructural attributes of base metal, heat affected zone and welded joints in both the welded plates were analyzed through optical microscope. The fractography analysis was conducted to get information about failure characteristics of samples after tensile testing. A significant change in mechanical properties, such as, 150% improvement in toughness, 7% reduction in weld-zone hardness, 3% improvement in yield strength and 6% reduction in ultimate tensile strength was obtained after tempering work. Also, the tempering process had reformed the grain structure by creating *twins* in base metal, and *lathy δ ferrite & γ+δ lamella* in HAZ. The martensite formed in quenched specimen had been completely recovered into fine γ+δ matrix. It was noticed that tempering had a potential to overcome all the disadvantages involved in quenching process.

Keywords: 304 SS; Heat treatment; Quenching; Tempering; Mechanical testing; Microstructure; Fractography

INTRODUCTION

Metallography has always been an interesting area of research. Many industries like construction, automobile, aerospace, and chemical plants require some specific metals with improved mechanical properties. Welding is one of the most important fabrication processes, although it is an old theory, but research is still continuously going on. The weldability of metals like aluminium, titanium alloys, and steels (and its different alloys) was extensively tested by metallurgist so that their applicability in industries can be enhanced [1-9]. Many heat treatment techniques were also discussed to improve the mechanical properties [10-14].

SS 304 is the most popular kind of stainless steel. The steel mostly alloyed with chromium and nickel (alloy elements between 8% and 10%) [15]. This kind of stainless steel is considered as austenitic steel. Compared to carbon steel, it is less thermally and electrically conductive. Also, it possesses lesser magnetism than carbon steel. Because it is simple to mould into different forms and has more corrosion resistance than normal steel, it is widely used. The nominal chromium and nickel contents of 304, 304H, and 304L are identical, hence they all have the same corrosion resistance, ease of manufacturing, and weldability. When exposed to various corrosive media and conditions, stainless steel 304 exhibits remarkable corrosion resistance. SS 304 can be easily joined by arc welding techniques like tungsten inert gas welding and metal inert gas welding. In past decades, SS 304 has been investigated for its weldability, joint strength, capabilities of dissimilar joints, and various other factors so that application of SS-304 can be enhanced. Some recent literatures have been reviewed as follows:

On welded plates of the medium carbon steel grade 55Si7, Krolicka et al. used a regeneration technique and heat treatments. The welded plates displayed a drop in hardness after the regenerative method, with the heat impacted zone showing the greatest reduction in hardness [16]. For welding and analysis, 120Mn3Si2 steel was employed by Brykov et al. The samples were cooled in water after welding. It was noted that the welded zone was where the austenitic layers originated. Additionally, residual austenite formed in layers, leading to martensite. Austenite layers were crucial in making the specimen tough during the toughness test. The welded joint's tensile strength was found to be 209.27 MPa, which is below average [17]. Ahonen et al. examined the results of thermal ageing at 400ºC in welds of different metals. It was discovered that heat ageing had increased carbon diffusion from the fusion boundary of weld metal to other parts of base metal side. The surface microstructure was composed primarily of martensite, with minor amounts of austenite and ferrite also present. In comparison to low carbon steel, the surface layer's hardness and

corrosion resistance were higher. The base material's and the stainless-steel surface layer's combined micro-hardness is less than that of the weld. The best corrosion resistance is found at the surface layer, and the welding seam has corrosion resistance that is better than the material beneath it [18]. SS 304 layer was deposited on Q235 low carbon steel by MIG technique to improve the mechanical properties of low-C steel. The results demonstrated that the welded joints and surface-modified plates did not possess any defects. Martensite dominated the microstructure of the surface layer, with trace levels of austenite and ferrite being present. The surface layer's hardness and corrosion resistance were greater than those of low carbon steel. The combined micro-hardness of the base material and the stainless-steel surface layer is lower than that of the weld. The surface layer exhibits the best corrosion resistance, and the welding seam exhibits corrosion resistance that is superior to the material below it [19].

In a work, the dissimilar metal joints were made between stainless steel (five different grades) and structural steel by using MIG. In order to assess the reliability of these welds, thorough microscopic and experimental examinations were carried out. MIG process settings were chosen correctly so that weld defects can be avoided. Tensile and hardness tests were used to evaluate how well dissimilar welds performed. Austenitic and martensitic steel welds with different hardness profiles later had very high heat-affected zone (HAZ) values caused fractures to form in this area during the tensile test. The average tensile strength was 472 MPa was measured. It was noted that usage of filler rod 308LSI was the best suited for joining structural steel and stainless steel [20]. An experiment was conducted to find an appropriate set of welding parameters for joining AISI 409L steel by pulsed current TIG welding technique. Taguchi method with L9 orthogonal array was employed for optimization. With pulsed TIG, Taguchi enhanced the surface shape, mechanical characteristics, and welding conditions for butts. The findings suggested that high-frequency pulsing with the right aspect ratio might penetrate completely. However, resultant % for both butt and TIG welds was found lesser than that of the base metal. The pulsed TIG welds' increased tensile strength and decreased ductility were attributed to martensitic growth. Since the zone for fusion is harder than the base metal, the hardness results also coincide with the results of the tensile tests. The corrosion behaviour of the source metal and the welded specimen was investigated using a potentio-dynamic polarisation method. The electrochemical behaviour of base material and weld samples indicates that the parent material has stronger overall corrosion resistance than the other zones. [21]. A research work on heat source model and weld profile was conducted for a laser-fiber welded SS-A304 plates. As per results, Gaussian heat source model cannot accurately represent the laser weld profile, which is the major issue with laser welding modelling. In the study, fibre laser butt welding was experimentally assessed on SS plate and then modelled using finite element analysis (FEA). Most studies take only bead diameter and penetration depth into account, which is improper for laser keyhole welding nails. Heat is the primary issue with laser welding modelling-The laser weld profile cannot be accurately reflected by a Gaussian heat source model. Additionally, fibre lasers are widely renowned for producing high-quality laser beam output, a lesser weld zone and good process efficiency when compared to other types of lasers (such as CO_2 and diode lasers) [22]. In a study, the conventional gas metal arc welding technique was altered to rotate the filler metal (wire) while feeding it downward, varying the fluid flow in the molten pool. Weld penetration was significantly reduced, and the weld microstructure was improved by the rotating fluid flow in the weld pool. The tensile strength of the weld metal was greatly boosted by the finer microstructure of the weld [23]. Five zones from the weld metal to the base metal were extensively examined to determine the microstructure, microhardness, and corrosion behaviour of a 2205 duplex stainless steel junction that was welded using double-pass tungsten inert gas arc welding with filler wire. According to the findings, reheating during second pass welding caused the development of significant amounts of secondary austenite in the weld metal and the emergence of coarse ferrite grains close to the fusion line, whereas other zones had comparable microstructures but different austenite concentrations. Additionally, it was noticed that the microhardness was influenced by the distribution of alloying elements (Chromium, Molybdenum, Nickel, and Nitrogen) and precipitates (chromium nitride). From the weld metal to the fusion line, austenite was tougher than ferrite; however, the strength of the two materials changed from the fusion line to the base metal [24]. A unique hybrid welding technique was used to effectively combine stainless steel and aluminium alloy. The steel side can be heated by the auxiliary TIG arc to change this behaviour. The decreased heat conductivity of steel can result in a significant change in temperature gradient on the steel surface during the MIG welding and brazing process. Additionally, the IMCs layer's Cr and Ni element content was raised, which can raise the layer's quality. The IMCs layer's microstructure was also enhanced, which strengthened the layer's adhesion to the weld seam. The use of the TIG enhanced the wettability of the molten metal, allowing it to spread completely across the front, rear, and upper surfaces of the steel and create a strong brazing junction. The joint's average tensile strength increased (to 146.7 MPa) with the auxiliary TIG arc compared to 96.7 MPa without it [25]. In a work, AISI 1018 steel samples were welded by friction stir (FSW) technique. The joints were analysed on the basis of tensile properties, fracture resistance, toughness values, hardness and microstructure. For performing FSW on 1018 steel, a tool with tungsten-mixed alloy was used in the study. The stir zone's tensile strength was found greater (8%) than the base metal. Due to the presence of tungsten particles in the weld area, the joints' ductility and impact toughness got reduced in comparison to those of the base metal [26]. In submerged arc welded (SAW) high strength low alloy steel, hardness was noticed to get significantly varied from weld center line to base metal zone. In welded zone, hardness was mostly uniform. The highest hardness was recorded in HAZ. Also, hardness had a negative effect by current. High amount of heat input was the result of coarse grain structure in HSLA plates. With an increase in current values, toughness was first increased to an extent. Later, it was reduced by providing excessive current [27].

According to this literature review, it has been derived that SS-304 steel are widely used and therefore a continuous assessment is being carried out to enhance its applicability. In this area, the present work describes a difference between quenching and tempering process over the welded plates of SS-304. The quality instruments for experimentation and microscopic analysis have been taken under study.

The objective of the present work is to examine the mechanical characteristics of welded joints made from 304 stainless steel plates that have undergone quenching and tempering treatment. Therefore, a comparison of the characteristics and microstructures of welded joints under the two different physical circumstances was made. The clear microstructural images provide a proper difference between quenching and tempering phenomena.

MATERIAL AND METHODS

Step-1: Collection of 304-SS plate: The SS-304 plates of dimension 50x50x3 mm were collected in 4 nos. The adjoining

plates were oriented in butt configuration. V groove of 60° was prepared on both upward and downward adjoining surfaces. They were joined by MIG welding technique by using SS filler wire (ER308). The diameter of electrode wire was 1.5 mm. The other technical specifications of MIG welding are written in step 2.

Step 2: Metal inert gas welding was used under study to weld SS plates. The voltage and current values of both the welded joints were kept same i.e., 20 V and 140 A respectively. A mixture of Ar (97.5%) and CO_2 (2.5%) gas was supplied to provide inert environment throughout the welded zone. The welding speed was 5 mm/s was maintained throughout the welding process.

Step 3: Heat treatment: (1) Both the welded plates were heated at 900ºC for 2 hours in an induction furnace. The prolonged heating at high temperature confirms restoration of internal stresses and refinement of microstructures. (2) After a required period of heating, the plates were quenched in water (25ºC). Both the plates took 1 min to get cooled up to room temperature; (3) Now, we have two 'Quenched' plates. Out of these two, one plate was again heated in the same furnace at 850ºC for 45 min and then allowed to get cooled in atmospheric air. It took nearly 2.5 hours to get cooled up to room temperature. (4) Finally, we have got two welded plates with two different physical conditions: (a) Quenched and (b) Tempered. The welding and heat-treating works are shown in **Fig. 1**.

Step 4: Tensile test specimen preparation: Both the welded plates were cut by wire-electric discharge machine so that necessary sized specimens for tensile test could be prepared. In this work, test specimens were prepared as per ASTM-E8 specifications. The test specimens are shown in **Fig. 2**. The tensile test was carried out on a hydraulically controlled Universal Testing Machine (UTM), named INSTRON 8800. The extension was done on a common strain rate of 0.001 s^{-1}. The broken samples after test are also shown in **Fig. 2**.

Step 5: Impact test specimen preparation: To know the toughness of welded joint in both the plates, Charpy impact test was carried out in the work. The sample size of 2.5×10×55 mm was considered for this test. The mid-part of the plate was cut by making a V notch of 30°. The specimen, in this test, is broken by imparting a sudden impact by a heavy hammer placed initially at 135° from vertical axis. As soon as the hammer is released, it suddenly applies fracture load on specimen and the energy absorbed by the specimen is indicated by the dial indicator. The prepared specimens, broken specimens, and readings of Charpy impact tester are shown in **Fig. 3**.

Step 6: Hardness test specimen preparation: For analyzing hardness of the specimen, Vickers hardness tester with 300 gm of load was used under study. Both the welded plates were finished properly (at cross sectional surface) so that no-unevenness should present to resist indentation during hardness test. Three different areas: base metal, heat affected, and welded zone were analyzed under hardness test.

Step 7: Preparation for Microstructure analysis: The microstructural analysis is a well-known technique used to assess the grain orientation in metals. As there were two different heat-treating approaches were followed in this work, the microstructural appearance must show the difference. Therefore, to know the difference in grain structure, the cross-sectional surface of the specimens was analysed for the microstructure observation. The surfaces were polished using different grades of sandpaper (100, 600, 1500, 2000, and 2200 grit sizes). A polishing machine was utilized to create a superfinished surface. The last step was to etch the samples using Nital solution (100 mL ethanol + 4 mL concentrated nitric acid), and then they were ready for the optical microscope. At a common magnification of 100x, three different zones, base metal, heat affected zone and welded zone were analyzed.

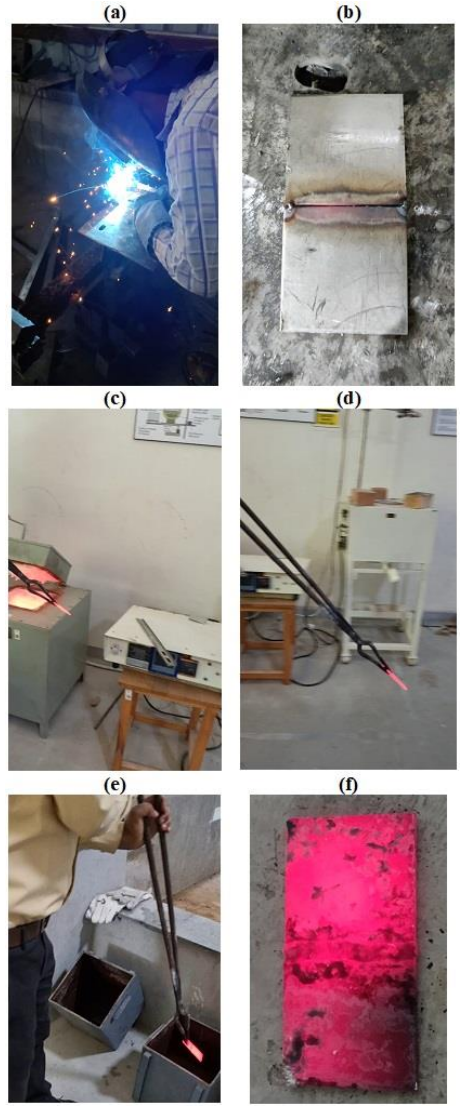

Fig. 1 (a, b) Welding of plates; (c, d) Heat Treatment; (e, f) Quenching and tempering.

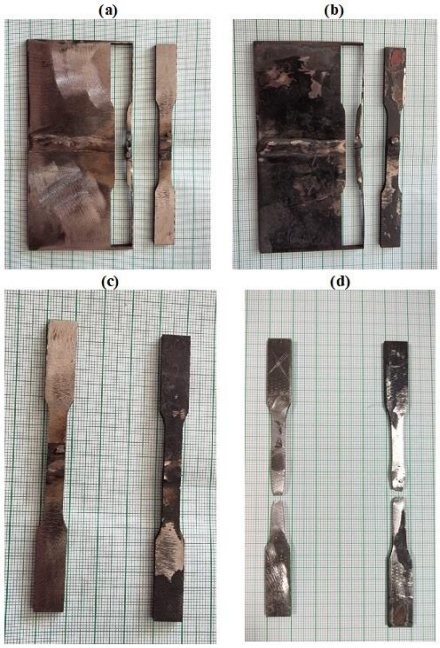

Fig. 2 (a, b, c) Cutting of ASTM specimens for tensile test; (d) Broken samples out of tensile test.

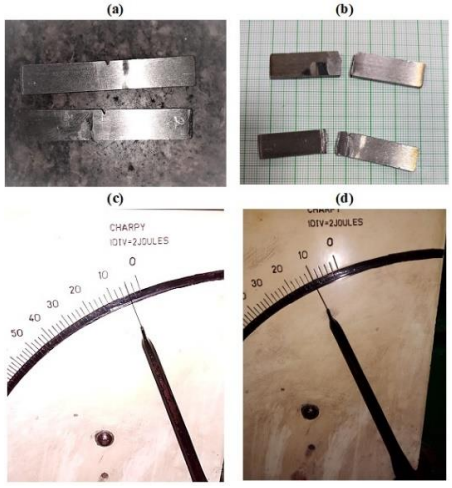

Fig. 3 (a) Specimens for impact test; (b) Broken samples after test; Dial indicators showing toughness values of (c) quenched and (d) tempered specimens.

RESULT ANALYSIS AND DISCUSSION

Analysis of Tensile Test results: The tensile stress vs strain graphs for both the welded specimens are shown in **Fig. 4** (a, b). Fig. 4(a) belongs to quenched specimen. It had taken 11.7 kN load to get fractured after an approximate elongation of 50%. The ultimate tensile strength (UTS) shown by quenched specimen is 694 MPa whereas the yield strength (YS) is 340 MPa. Fig. 4(b) belongs to tempered specimen in which the maximum load was reached up to 10.8 kN. The UTS and YS of the same is 654 MPa and 348 MPa respectively. The UTS of tempered specimen is nearly 6% lower than that of quenched specimen whereas the YS of the tempered specimen was found to increase by 3%. Also, the elongation shown by tempered specimen (38%) is lower than quenched product. The outcomes of tensile test are shown in **Table 1**.

Table 1 Outcomes of Tensile test

Sr. No.	SAMPLE NAME	Load (in kN)	Elongation (%)	Ultimate Tensile Strength	Yield Strength
1	Quenched	11.7	50	694 MPa	340 MPa
2	Tempered	10.8	38	654 MPa	348 MPa

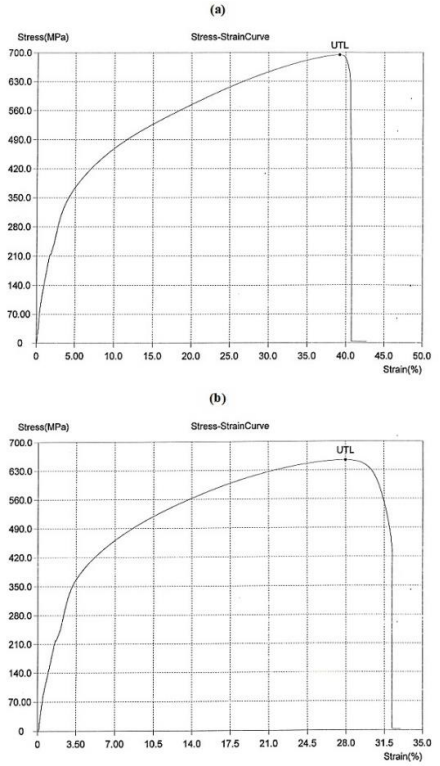

Fig. 4 Stress- Strain curve of (a) Quenched specimen; (b) Tempered specimen.

Fractographic analysis of broken tensile specimens: Through macroscopical examination, it was noticed that each specimen had failed by developing a cup-cone form, a sign of ductile failure. In order to further examine the fracture properties, fractographic experiments were carried out.

Fractographic analysis was performed to determine if the fracture is brittle or ductile in nature and to analyze the fracture behaviour of the tensile test specimens. For this purpose, all the broken specimens were cut from 5 mm below the fractured

surface. Each sample was observed through field emission scanning electron microscopy (FESEM). The fractographic images are shown in **Fig. 5** (a, b). Both the samples possessed similar kind of morphologies i.e, micro-dimples, and pores with no appearance of facets. Means, both the specimens showed a ductile failure across the welded joint. The tempered specimen imparts comparatively higher number of micro-dimples and pores.

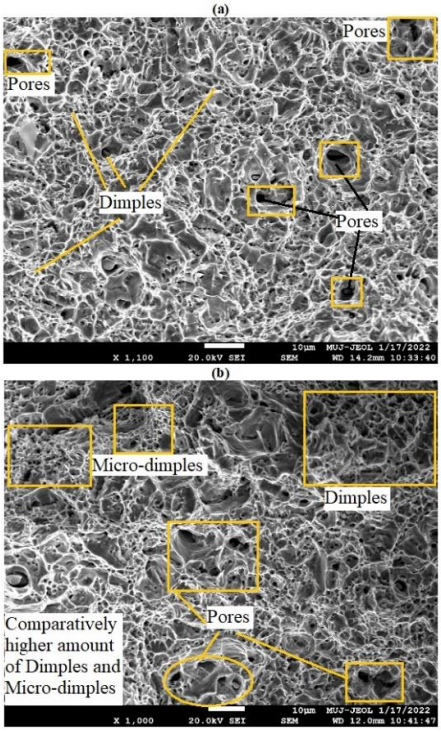

Fig. 5 Fractographic images of tensile test specimens: (a) of quenched specimen; (b) of tempered specimen.

Toughness test analysis: The toughness values of the quenched and tempered specimens were remarkably different. The quenched specimen got broken through heat affected zone (as per macroscopic observation) and tempered specimen failed through the welded part. Means, in quenched specimen, HAZ is the weakest part due to possessing residual stresses. The values of toughness in both the plates are shown in **Table 2**. The observation is showing very less values of toughness means probably there is some experimental defects in the specimens. However, the results shows that tempered specimen possesses 150% toughness value than quenched specimen.

Table 2 Impact test observations

Sr. No.	SAMPLE NAME	Measured Toughness (J)
1	Quenched Specimen	4
2	Tempered Specimen	10

Result analysis of hardness test: As per the micro-Vickers hardness test, the values of hardness at three different zones are discussed in **Table 3** and **Table 4**. It can be seen that an average hardness values at base metal, HAZ and welded zone in quenched specimens are 240 HV, 262 HV, and 458 HV respectively. The tempered specimen showed the hardness of 217 HV, 244 HV, and 429 HV in base metal, HAZ and welded zone respectively. The trend of hardness in both the samples is: Base metal < HAZ < Welded zone. In all the three zones, the quenched specimen possessed higher hardness than tempered one. A bar chart is shown in **Fig. 6** to compare hardness between two specimens.

Table 3 Hardness test results of Quenched specimen

Sr. No.	Zone	Hardness in HV	Average hardness (HV)
1	Base metal	241, 233, 245	240
2	HAZ	264, 253, 267	262
3	Welded zone	432, 464, 476	458

Table 4 Hardness test results of Tempered specimen

Sr. No.	Zone	Hardness in HV	Average hardness (HV)
1	Base metal	216, 209, 224	217
2	HAZ	243, 241, 248	244
3	Welded zone	432, 424, 429	429

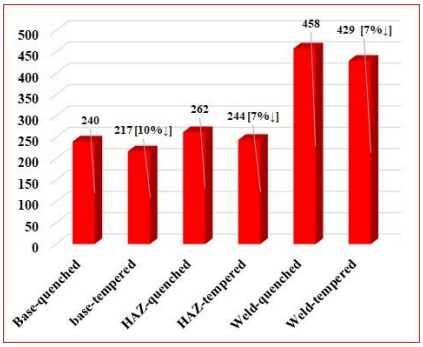

Fig. 6 Comparative analysis among hardness at different zones.

Microstructural analysis: The microscopic images of quenched and tempered welded specimens are shown in **Fig. 7** and **Fig. 8** respectively. In both the images, three zones i.e., Base metal (BM), Heat affected zone (HAZ) and Welded zone (WZ) were analyzed. As 304 grade SS is an austenitic steel, the base metal mainly imparts austenite (γ) matrix along with δ-ferrite (in skeletal or lathy form). The appearance of γ matrix is bright whereas δ-ferrite is having a black colored appearance. The base metal of quenched specimen contains coarse γ-matrix with no clearly visible twins over there.

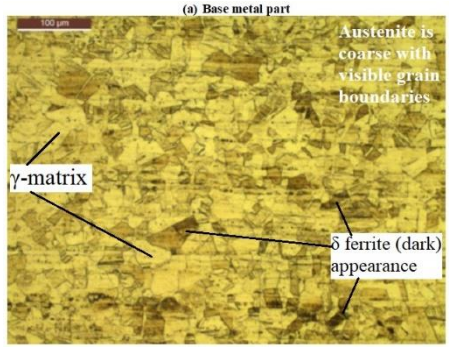

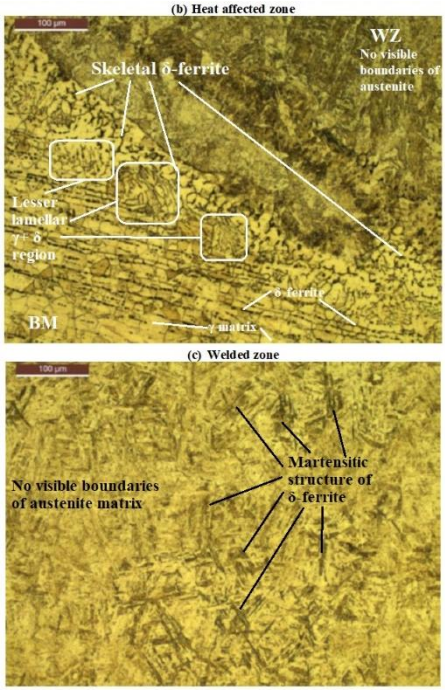

Fig. 7 Microstructure of quenched specimen: (a) Base metal; (b) HAZ; (c) Welded zone.

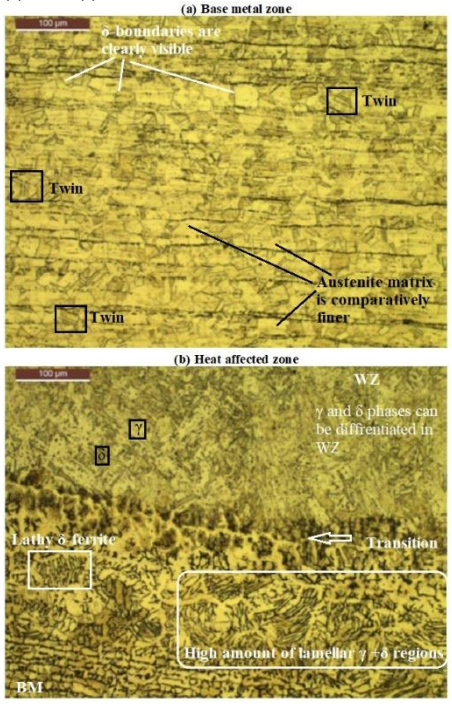

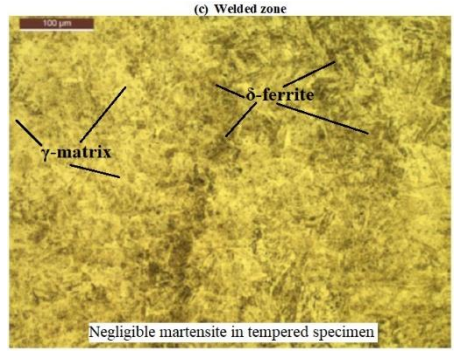

Fig. 8 Microstructure of tempered specimen: (a) Base metal; (b) HAZ; (c) Welded zone.

The HAZ or more specifically transition zone between BM and WZ mainly showed two kinds of structures- skeletal δ-ferrite [28] and γ+δ lamella [28]. skeletal δ-ferrite is predominant whereas lamellar γ+δ is less. The formation of γ+δ lamella is mainly towards the BM zone. Again, in the same image, γ and δ ferrite can be recognized according to their distinct appearance. In the welded zone (WZ), the original coarse appearance of austenite γ-matrix is lost. Also, there is no defined δ-ferrite in the same. They can be differentiated by their appearance- bright (γ) or dark (δ). Due to very fast rate of cooling, δ-ferrite has converted into acicular martensite in WZ. Due to presence of martensite, the WZ of quenched specimen is reported as highly hard (458 HV).

As compared with quenched specimen, the microstructural appearance of tempered specimen is different. Grain size is refined after tempering. The BM carries comparatively finer γ matrix with approximately an equiaxed δ-ferrite. The γ-matrix is having clearly visible grain boundaries. Unlike quenched specimen, multiple twins can be observed in γ-matrix. The HAZ is also having a different structure than in quenched product. Some lathy δ-ferrites were reported (shown inside white rectangle) along with high amount of γ+δ lamella. The WZ carries two distinct γ and δ phases. Unlike quenched specimen, the tempered specimen does not possess acicular martensite structure. However, fine (dark in color) δ ferrite regions were reported in the same. The fine microstructures in the welded zone make it harder than other two zones (BM and HAZ).

CONCLUSIONS

An attempt has been made to analyze the mechanical properties and microstructure of SS-304 welded plates welded by MIG technique. Two such welded plates were taken and then they were heat treated. Initially, both the plates were quenched and then one of the samples was tempered. In this way, two welded plates were achieved in two different physical conditions. Both the plates were analyzed and compared with regard to tensile strength, hardness and impact strength. Also, the microstructural analysis was carried out to know the exact material behavior. This work can be concluded as follows:

- As per the tensile test results, tempering process has reduced the UTS by 6% with an improvement in YS by 3%. Although the quantitative changes are not too significant, the fractographic images shows a remarkable difference between the two specimens. The tempered specimen possesses a higher

number of pores and micro-dimples than these of quenched one.

- The toughness value of tempered specimen is 150% higher than quenched specimen. It might be due to difference in fracture zone. Quenched specimen got fractured through HAZ which is the weakest part of the plate. The tempered specimen got fractured through the welded joint.
- As expected, quenched specimen was reported as harder than tempered one. The % reductions in hardness at BM, HAZ, and WZ of tempered specimen are 10%, 7%, and 7% respectively. In both the specimens the hardness trend in all the three zones is similar, i.e., hardness of WZ > hardness of HAZ > hardness of BM.
- Quenched and tempered specimens have different microscopic appearance. In quenched specimen, mainly coarse γ matrix with δ-ferrite was reported in BM; skeletal-δ with a little γ+δ lamella was reported in HAZ; a very fine γ-matrix with martensitic- δ ferrite was observed in WZ. In tempered specimen, fine γ+δ matrix was observed in BM; lathy δ-ferrite with many γ+δ lamella were reported in HAZ; very fine γ matrix (along with δ) but no martensite was recognized in WZ.
- The mechanical properties are in good corroboration with microstructural attributes. No formation of martensite in the WZ of tempered product proves the successful heat treatment on the sample.
- The present experimental work has been accomplished with a successful improvement in mechanical properties with an adequate grain refinement.

REFERENCES

1. T.S. Balasubramanian, M. Balakrishnan, V. Balasubramanian, M.M. Manickam: Transactions of Nonferrous Metals Society of China, 21(6), 2011, 1253–1262. https://doi.org/10.1016/S1003-6326(11)60850-9.
2. D.K. Gope, U. Kumar, S. Chattopadhyaya, S. Mandal: Journal of Mechanical Science and Technology, 32(6), 2018, 2715–2721. https://doi.org/10.1007/s12206-018-0528-7.
3. G. Lütjering, J.C. Williams, A. Gysler: Microstructure and mechanical properties of titanium alloys. In Microstructure And Properties Of Materials 2, 2000, 1–77. https://doi.org/10.1142/9789812793959_0001.
4. J. Józwik, D. Ostrowski, R. Milczarczyk, G. Krolczyk: Journal of the Brazilian Society of Mechanical Sciences and Engineering, 40(215), 2018. https://doi.org/10.1007/s40430-018-1144-2.
5. U. Kumar, D. K. Gope, R. Kumar, S. Chattopadhyaya, A.K. Das, A. Pramanik, G. Krolczyk: Metallic Materials/Kovové Materiály, 56(2), 2018, 121–129. https://doi.org/10.4149/km_2018_2_121.
6. G. Krolczyk, A. Sedmak, U. Kumar, S. Chattopadhyaya, A.K. Das, A. Pramanik: Natural Resources & Engineering, 1(2), 2016, 51–58. https://doi.org/10.1080/23802693.2016.1246278.
7. S. Shankar, K. Saw, S. Chattopadhyaya, S. Hloch: Materials Today: Proceedings, 5, 2018, 24378–24386. https://doi.org/10.1016/j.matpr.2018.10.233.
8. R. Kumar, B. Bora, S. Chattopadhyaya, G. Krolczyk, S. Hloch: Int. J. Materials and Product Technology, 57(1/2/3), 2018, 204-229. DOI: 10.1504/IJMPT.2018.092920
9. R. Kumar, S. Chattopadhyaya, A.R. Dixit, B. Bora, M. Zelenak, J. Foldyna, S. Hloch, P. Hlavacek, J. Scucka, J. Klich, L. Sitek: The International Journal of Advanced Manufacturing Technology, 88(5-8), 2017, 1687-1701. https://doi.org/10.1007/s00170-016-8776-0.
10. S. Dewangan, S.K. Mohapatra, A. Sharma: Grey Systems: Theory and Application, 10(3), 2020, 281–292. https://doi.org/10.1108/GS-11-2019-0052.
11. S. Dewangan, M.R. Patel, R. Singh, A. Kumar, D.K. Gope, U. Kumar: AIP Conference Proceedings, 2148(1), 2019, 030043. https://doi.org/10.1063/1.5123965.
12. S. Dewangan, S. Behera, M.K. Chowrasia: World Journal of Engineering, 17(1), 2020, 127–133. https://doi.org/10.1108/WJE-11-2019-0327.
13. S. Dewangan, N. Mainwal, M. Khandelwal, P.S. Jadhav: Australian Journal of Mechanical Engineering, 20(1), 2022, 74-87. https://doi.org/10.1080/14484846.2019.1664212.
14. U. Kumar, D. Gope, J. Srivastava, S. Chattopadhyaya, A. Das, G. Krolczyk: Materials, 11(9), 2018, 1514. https://doi.org/10.3390/ma11091514.
15. W. D. Callister, D. G. Rethwisch: *Materials Science and Engineering: An Introduction*, 10th Edition, John Wiley and Sons, New York, 2018. ISBN: 978-1-119-40549-8
16. A. Królicka, K. Radwański, A. Janik, P. Kustroń, A. Ambroziak: Materials, 13(21), 2020, 4841. https://doi.org/10.3390/ma13214841.
17. M.N. Brykov, I. Petryshynets, M. Džupon, Y.A. Kalinin, V.G. Efremenko, N.A. Makarenko, D.Y. Pimenov, F. Kováč: Materials, 5059, 2020, 13. https://doi.org/10.3390/ma13225059.
18. M. Ahonen, R. Mouginot, T. Sarikka, S. Lindqvist, Z. Que, U. Ehrnstén, I. Virkkunen, H. Hänninen: Metals, 10, 2020, 421. https://doi.org/10.3390/met10030421.
19. T. Wang, S.S. Ao, S. M. Manladan, Y.C. Cai, Z. Luo: Materials, 12, 2019, 2883. https://doi.org/10.3390/ma12182883.
20. S. Baskutis, J. Baskutiene, R. Bendikiene, A. Ciuplys, K. Dutkus: Materials, 14, 2021, 6180. https://doi.org/10.3390/ma14206180.
21. K. B. Behredin, P. J. Ramulu, B. Habtamu, N. Besufekad, N. Tesfaye: Advances in Materials Science and Engineering, volume 2022, Article ID 8276496, 2022, 16 pages. https://doi.org/10.1155/2022/827649627.
22. L. Peizhi, Y. Fan, C. Zhang, Z. Zhu, W. Tian, A. Liu: Advances in Materials Science and Engineering, volume 2018, Article ID 5895027, 2018, 12 pages. https://doi.org/10.1155/2018/5895027.
23. H. Zhang, Q. Chang, J. Liu, H. Lu, H. Wu, J. Feng: Materials Letters, 123, 2014, 101–103. https://doi.org/10.1016/j.matlet.2014.03.018.
24. S. Geng, J. Sun, L. Guo, H. Wang: Journal of Manufacturing Processes, 19, 2015, 32–37. https://doi.org/10.1016/j.jmapro.2015.03.009.
25. H. Zhang, J. Liu, J. Feng. Trans. Nonferrous Met. Soc. China, 24, 2014, 2831−2838. https://doi.org/10.1016/S1003-6326(14)63415-4
26. A. K. Lakshminarayanan, V. Balasubramanian, M. Salahuddin: Journal of Iron and Steel Research, International, 17(10), 2010, 68-74. https://doi.org/10.1016/S1006-706X(10)60186-0
27. K. Prasad, D. K. Dwivedi: Int J Adv Manuf Technol, 36, 2008, 475–483. https://doi.org/10.1007/s00170-006-0855-1.
28. J. W. Fu, Y. S. Yang, J. J. Guo, J. C. Ma, W. H. Tong: Materials Science and Technology, 25(8), 2009, 1013-1016. https://doi.org/10.1179/174328408X317093.